Dynamical Casimir effect via modulated Kerr or higher-order nonlinearities

A. V. Dodonov * and V. V. Dodonov †

Institute of Physics, University of Brasilia, P. O. Box 04455, 70919-970 Brasilia, Federal District, Brazil and International Centre of Physics, University of Brasilia, 70297-400 Brasilia, Federal District, Brazil

(Received 20 August 2021; accepted 3 January 2022; published 14 January 2022)

We show two examples in which the dynamical Casimir effect can be achieved by modulating the Kerr or higher-order nonlinearities. In the first case the cavity field is coupled to an arbitrary number of qubits or a harmonic oscillator via the dipole interaction. In the second case, the modulation of the nonlinearities is accompanied by the off-resonance modulation of the cavity frequency. We present the analytic description of the phenomenon and supplement it with numeric simulations, demonstrating that photons can be created from vacuum and the resulting hyper-Poissonian photon statistics is very different from the squeezed vacuum state.

DOI: 10.1103/PhysRevA.105.013709

I. INTRODUCTION

A possibility of creating quanta of the electromagnetic field from the initial vacuum state in cavities with moving boundaries, first predicted by Moore [1] and called nowadays as the dynamical Casimir effect (DCE), was a subject of numerous studies for several decades (see, e.g., the reviews [2–6]). However, until now it seems impossible to observe the effect in its "pure" form, due to small velocities (compared with the speed of light) of real boundaries that could be achieved in a laboratory. Therefore, the idea of *simulating* this motion in more simple arrangements, resulting in the parametric amplification of vacuum fluctuations, was considered for a long time by many authors [7–14]. Such phenomena can be called the *parametric DCE* (or PDCE). One of possibilities is to use some electrical circuits (waveguides) with distributed or lump elements, whose parameters (e.g., capacitance, inductance, magnetic flux, critical current, etc.) could be made time dependent [9,15–17]. The idea to use a superconducting coplanar waveguide in combination with a Josephson junction was developed in [18–21], and the experiments were reported in [22–25]. Further improvements of experimental schemes were suggested in [26–34]. In particular, the circuit QED with "artificial atoms" (qubits) was the subject of studies [35–46].

Although the simplest models predict an exponential growth of the number of quanta created from vacuum under the DCE parametric resonance conditions [2], realistic numbers can be limited due to many factors. One such factor is related to unavoidable nonlinearities in real systems [47–51]. As a rule, nonlinearities with time-independent parameters play a negative role, leading the system out of resonance, thus diminishing the number of quanta that could be created from vacuum. The aim of our paper is to show that *time-modulated* nonlinear effects can be used to create photons from vacuum, resulting in new quantum states of the electromagnetic field (quite different from the typical squeezed vacuum state generated in the linear parametric amplification processes). Namely, we assume that the Hamiltonian has the form (hereafter $\hbar = 1$ and $\eta > 0$)

$$\hat{H} = \varepsilon \sin(\eta t)\hat{n}^k + \hat{H}_0, \tag{1}$$

where $\hat{n} = \hat{a}^\dagger \hat{a}$ is the photon number operator ($\hat{a}$ and $\hat{a}^\dagger$ being the standard annihilation and creation operators) and $k \geqslant 2$ is an integer (the case $k = 1$, corresponding to the modulation of the cavity frequency, was thoroughly studied previously in [38,39]). ε is the amplitude of modulation of the nonlinearity, while η is the modulation frequency. We consider two examples of the "bare" Hamiltonian $\hat{H}_0$. The first one (Sec. II) describes the interaction of the field mode with a chain of qubits or a harmonic oscillator, whereas the second one corresponds to a nonresonantly modulated cavity (Sec. III). A discussion of the results appears in Sec. IV.

II. EMPLOYING DISPERSIVE QUBITS

In this section, we consider the bare Hamiltonian $\hat{H}_0$ describing the *quantum Dicke model* [52,53] including a Kerr nonlinearity with a constant strength α (whose role is to minimize the qubit-induced nonlinearity, as will be seen shortly), $\hat{H}_0 = \omega\hat{n} + \alpha\hat{n}^2 + \hat{H}_1$, where

$$\hat{H}_1 = \sum_{l=1}^{N}\left[\frac{\Omega}{2}\hat{\sigma}_z^{(l)} + g(\hat{a} + \hat{a}^\dagger)(\hat{\sigma}_+^{(l)} + \hat{\sigma}_-^{(l)})\right]. \tag{2}$$

Here ω is the constant cavity frequency, Ω is the constant atomic transition frequency, g is the atom-field coupling constant, and N is the number of identical noninteracting atoms. The qubit operators are $\hat{\sigma}_-^{(l)} = |g^{(l)}\rangle\langle e^{(l)}|$, $\hat{\sigma}_+^{(l)} = |e^{(l)}\rangle\langle g^{(l)}|$, and $\hat{\sigma}_z^{(l)} = |e^{(l)}\rangle\langle e^{(l)}| - |g^{(l)}\rangle\langle g^{(l)}|$, where $|g^{(l)}\rangle$ and $|e^{(l)}\rangle$ denote the ground and excited states of the lth qubit, respectively. The Hamiltonian (2) is the starting point in the studies devoted to the interaction of a single mode of the electromagnetic field with ensembles of two-level objects ("qubits").

*adodonov@unb.br
†vdodonov@fis.unb.br

To obtain a closed analytical description we employ the normalized *Dicke* states with k atomic excitations (denoted by a bold index) [52,53]

$$|\mathbf{k}\rangle = \sqrt{\frac{k!(N-k)!}{N!}} \sum_p |e^{(1)}\rangle \cdots |e^{(k)}\rangle |g^{(k+1)}\rangle \cdots |g^N\rangle,$$

where the sum runs over all allowed permutations of excited and nonexcited qubits and $k = 0, 1, \ldots, N$. In terms of the collective qubit operators $\hat{\sigma}_{k,j} \equiv |\mathbf{k}\rangle\langle\mathbf{j}|$ we have

$$\hat{H}_1 = \sum_{k=0}^{N} [k\Omega\hat{\sigma}_{k,k} + g f_k(\hat{a} + \hat{a}^\dagger)(\hat{\sigma}_{k,k+1} + \hat{\sigma}_{k+1,k})], \qquad (3)$$

where $f_k \equiv \sqrt{(k+1)(N-k)}$. Hamiltonian (3) can be simplified if $N \gg 1$ and the maximum number of atomic excitations is small compared to the number of atoms ($k_{\max} \ll N$). Writing $g = g_{ho}/\sqrt{N}$ and taking the limit $N \to \infty$ one can arrive at the Hamiltonian of two coupled harmonic oscillators,

$$\hat{H}_1 = \Omega\hat{b}^\dagger\hat{b} + g_{ho}(\hat{a} + \hat{a}^\dagger)(\hat{b} + \hat{b}^\dagger), \qquad (4)$$

where $\hat{b} = \sum_{k=0}^{\infty} \sqrt{k+1}\hat{\sigma}_{k,k+1}$ is the collective atomic operator, satisfying the standard bosonic commutation relation $[\hat{b}, \hat{b}^\dagger] = 1$.

In the presence of the nonlinear term in the total Hamiltonian $\hat{H}$ (1), it is convenient [45,54] to expand the wave function as

$$|\psi\rangle = \sum_n \exp\left[(i\varepsilon\xi_n/\eta)\cos(\eta t) - \mathrm{i}t\lambda_n\right] c_n(t)|\varphi_n\rangle, \qquad (5)$$

where $\xi_n = \langle\varphi_n|\hat{n}^k|\varphi_n\rangle$ and $|\varphi_n\rangle$ is the eigenstate (dressed state) of $\hat{H}_0$ with the eigenvalue λ_n; the sum runs over all the dressed states, with the index n increasing with energy (i.e., $\lambda_{n+1} \geqslant \lambda_n$). After substituting Eq. (5) into the Schrödinger equation, one finds that the probability amplitudes of the dressed states, c_n, obey the set of differential equations

$$i\dot{c}_m = 2\sin(\eta t) \sum_{n\neq m} \exp\left[iQ_{mn}\cos(\eta t) - it\lambda_{nm}\right] R_{mn}c_n, \qquad (6)$$

where $\lambda_{nm} = \lambda_n - \lambda_m$ and

$$Q_{mn} \equiv (\varepsilon/\eta)(\xi_n - \xi_m), \quad R_{mn} \equiv (\varepsilon/2)\langle\varphi_m|\hat{n}^k|\varphi_n\rangle. \qquad (7)$$

Using the Jacobi-Anger expansion

$$\exp[iz\cos(x)] = J_0(z) + 2\sum_{l=1}^{\infty} i^l J_l(z)\cos(nx)$$

together with the recurrence relation

$$J_{l-1}(z) + J_{l+1}(z) = 2lz^{-1}J_l(z),$$

one can rewrite Eq. (6) in terms of the Bessel functions of the first kind:

$$\dot{c}_m = -4\sum_{n\neq m} R_{mn}c_n e^{-it\lambda_{nm}} \sum_{l=1}^{\infty} l i^l \frac{J_l(Q_{mn})}{Q_{mn}} \sin(l\eta t). \qquad (8)$$

The equivalent sets of Eqs. (6) and (8) are exact but rather complicated. However, they can be simplified significantly under the condition $|Q_{mn}| \ll 1$ (which is satisfied for typical experimental situations). The right-hand side of Eq. (8) exhibits fast oscillations as a function of time, which averages to zero, unless the modulation frequency assumes resonant values $\eta \approx |\lambda_{nm}|/l$ simultaneously with nonzero R_{mn}. In this case, the external perturbation drives the transition between the dressed states $\{\varphi_m, \varphi_n\}$; since the modulation frequency is controlled externally, the order l of the resonance and the coupled states are chosen by the experimentalist. In the realistic scenario $lJ_l(Q_{mn})R_{mn}/Q_{mn} \ll l\eta + |\lambda_{nm}|$ for the relevant values of m, n, and l, one can neglect rapidly oscillating terms to obtain

$$\dot{c}_m = \sum_{n\neq m} \theta_{mn}R_{mn}c_n \sum_{l=1}^{\infty} l i^{l-1} \frac{2J_l(Q_{mn})}{Q_{mn}} e^{it\theta_{mn}(|\lambda_{nm}| - l\eta)},$$

where $\theta_{mn} = \mathrm{sgn}(\lambda_{mn})$. Since $J_n(x) \approx x^n/(2^n n!)$ for $|x| \ll 1$, we have $2lJ_l(Q_{mn})/Q_{mn} \approx Q_{mn}^{l-1}/[2^{l-1}(l-1)!]$ if $|Q_{mn}| \ll 1$. Therefore, the benefit of using higher-order resonances is offset by much lower transition rates [39]. For simplicity, here we focus on the lowest-order resonance $l = 1$. In this case, the exact set of equations can be replaced with a simpler one,

$$\dot{c}_m = \sum_{n\neq m} \theta_{mn}R_{mn}c_n \exp\left[it\theta_{mn}(|\lambda_{nm}| - \eta)\right]. \qquad (9)$$

Only the terms satisfying the resonance condition $|\lambda_{nm}| \approx \eta$ simultaneously with nonzero R_{mn} make the main contribution to the right-hand side of this equation. We also notice that the above approximation introduces small shifts [35] to the resonant modulation frequency $|\lambda_{nm}|$, which are more easily found numerically.

For the scope of this work it is sufficient to work in the dispersive regime and weak Kerr nonlinearity: $gf_k\sqrt{n}$, $2|\alpha|n \ll |\omega - \Omega|$ for all relevant values of n and k. In this regime one can find the eigenstates of $\hat{H}_0$ via the standard nondegenerate perturbation theory. Since DCE concerns the generation of photon pairs from vacuum, we only need the dressed states in which the atoms remain approximately in the collective ground state $|\mathbf{0}\rangle$. To the second order in g these (non-normalized) eigenstates read

$$\begin{aligned}
|\varphi_n\rangle = {} & |\mathbf{0}, n\rangle + \frac{g\sqrt{Nn}}{\omega - \Omega}|\mathbf{1}, n-1\rangle \\
& - \frac{g\sqrt{N(n+1)}}{\omega + \Omega}|\mathbf{1}, n+1\rangle \\
& + \frac{Ng^2\sqrt{n(n-1)}}{2\omega(\omega - \Omega)}|\mathbf{0}, n-2\rangle \\
& + \frac{g^2N\sqrt{(n+1)(n+2)}}{2\omega(\omega + \Omega)}|\mathbf{0}, n+2\rangle \\
& + \frac{g^2\sqrt{2Nn(N-1)(n-1)}}{2(\omega - \Omega)^2}|\mathbf{2}, n-2\rangle \\
& + \frac{g^2\sqrt{2N(N-1)}[\omega - \Omega(2n+1)]}{2\Omega(\omega^2 - \Omega^2)}|\mathbf{2}, n\rangle \\
& + \frac{g^2\sqrt{2N(N-1)(n+1)(n+2)}}{2(\omega + \Omega)^2}|\mathbf{2}, n+2\rangle. \qquad (10)
\end{aligned}$$

The dressed states with excited atoms can be found similarly, but they are not important here.

The energy difference between the dressed states differing by (roughly) two photons reads

$$\frac{\lambda_{n+2}-\lambda_n}{2} \approx \omega + 2\alpha + 2n\left[\alpha + \frac{2\Omega g^4 N(\omega^2+3\Omega^2)}{(\Omega^2-\omega^2)^3}\right] - \frac{2\Omega N g^2}{\Omega^2-\omega^2}\left[1 - g^2\frac{3\omega(\omega^2+3\Omega^2)+\Omega[(5N-8)\omega^2 - N\Omega^2]}{\omega(\Omega^2-\omega^2)^2}\right].$$

By adjusting the static value of the Kerr nonlinearity to

$$\alpha_0 = -\frac{2\Omega g^4 N(\omega^2+3\Omega^2)}{(\Omega^2-\omega^2)^3},$$

this energy difference becomes independent of the photon number to the fourth order in g:

$$\frac{\lambda_{n+2}-\lambda_n}{2} \approx \omega - \frac{2\Omega N g^2}{\Omega^2-\omega^2}\left[1 - g^2\frac{\omega(\omega^2+3\Omega^2)+\Omega[(5N-8)\omega^2 - N\Omega^2]}{\omega(\Omega^2-\omega^2)^2}\right]. \tag{11}$$

Therefore, all the low-lying dressed states (satisfying $gf_k\sqrt{n} \ll |\omega-\Omega|$) *can be coupled resonantly by a single-tone modulation*. This means a possibility of the photon creation from vacuum via the modulation of nonlinearities. However, the dynamics of this process is different from the standard DCE (when the time-dependent interaction Hamiltonian is proportional to $\hat{a}^{\dagger 2} + \hat{a}^2$ [55]), as well as from the case when the photon generation can be achieved via the modulation of parameters Ω or g [18,35,36,38,56]. To show the origin of the difference, let us analyze the structure of matrix elements (7) determining the evolution through the set of equations (6). Under the assumptions made before, these matrix elements can be written as follows:

$$Q_{n,n+2} \approx (\varepsilon/\eta)[(n+2)^k - n^k],$$

$$R_{n,n+2} = \frac{N\varepsilon(g/\omega)^2}{2(\nu^2-1)}\sqrt{(n+1)(n+2)}M_k(n,\nu), \tag{12}$$

$$M_k(n,\nu) = (n+1)^k - \frac{1-\nu}{2}(n+2)^k - \frac{1+\nu}{2}n^k, \tag{13}$$

where $\nu = \Omega/\omega$. For the realistic case $2kn_{\max}^{k-1}\varepsilon \ll \eta$ (where $n_{\max}$ is the maximum relevant photon number) one has $Q_{n,n+2} \ll 1$, so the actual transition rate between the states $|\varphi_n\rangle$ and $|\varphi_{n+2}\rangle$ is given by the coefficient $R_{n,n+2}$ [this means, in particular, that Eq. (9) is indeed an excellent approximation to Eq. (8)]. Moreover, since the above results were derived assuming that the atoms remain predominantly in the ground states (so the condition $k_{\max} \ll N$ is fulfilled), we can immediately infer the results for the harmonic oscillator by making the substitution $g = g_{ho}/\sqrt{N}$ and then taking the limit $N \to \infty$ (in this case $\alpha_0 = 0$, therefore the static Kerr term is not required).

As shown in previous papers [18,35,36,38,55,56], the transition rate $R_{n,n+2}$ scales as $\sqrt{(n+1)(n+2)}$ for the modulation of parameters Ω or g, as well as in the standard DCE. On the other hand, Eq. (12) contains an extra factor $M_k(n,\nu)$ (13). Only $M_1 = 2\nu$ does not depend on the quantum number n. This situation corresponds to the "standard DCE case" (i.e., the modulation of the cavity eigenfrequency). All coefficients M_k with $k \geqslant 2$ depend on n. In particular,

$$M_2 = 2(n+1)\nu - 1, \quad M_3 = (3n^2+6n+4)\nu - 3(n+1).$$

Therefore, one can expect that the dynamics in the case of $k \geqslant 2$ can be different from the cases studied earlier. This conjecture is confirmed numerically in the following section.

Numeric results for a single qubit

The analytic results (11)–(13) were deduced for a weak atom-field coupling strength g, when the transition rate $R_{n,n+2} \propto (g/\omega)^2$ is also small. However, to observe the predicted phenomenon experimentally, the circuit QED architecture is the most promising candidate, and there the parameter g can be easily made as large as 0.1ω [57,58], while the Kerr nonlinearity can also be modulated externally in real time [59]. In this regime, it is easier to evaluate the transition rate $R_{n,n+2}$ and the resonant modulation frequencies by diagonalizing numerically the Hamiltonian $\hat{H}_0$, since the system dynamics is still described by Eq. (8). This is done in Fig. 1. In Fig. 1(a) the solid lines illustrate the ratio of matrix elements $r_n \equiv R_{n,n+2}/R_{0,2}$ obtained by exact numeric diagonalization of the Hamiltonian (2) for $N = 1$ and parameters $k = 2$, $\alpha = 0$, and $g/\omega = 0.07$. The condition $gf_k\sqrt{n} \ll |\omega-\Omega|$ is not satisfied in this regime of parameters, so the approximate expressions (12) and (13) do not hold. The dashed lines illustrate

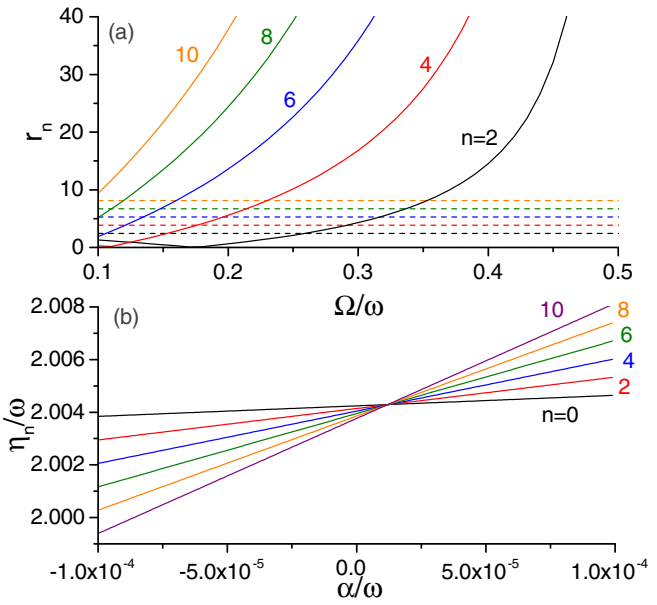

FIG. 1. (a) Ratio of the transition rates $r_n = R_{n,n+2}/R_{0,2}$ as a function of Ω/ω. Solid lines indicate r_n for $k = 2$ (modulation of Kerr nonlinearity); dashed lines indicate r_n for the standard DCE (when $k = 1$). (b) Energy differences $\eta_n = \lambda_{n+2} - \lambda_n$ between adjacent dressed states as functions of the (relative) static Kerr nonlinearity α/ω for $\Omega/\omega = 0.21$.

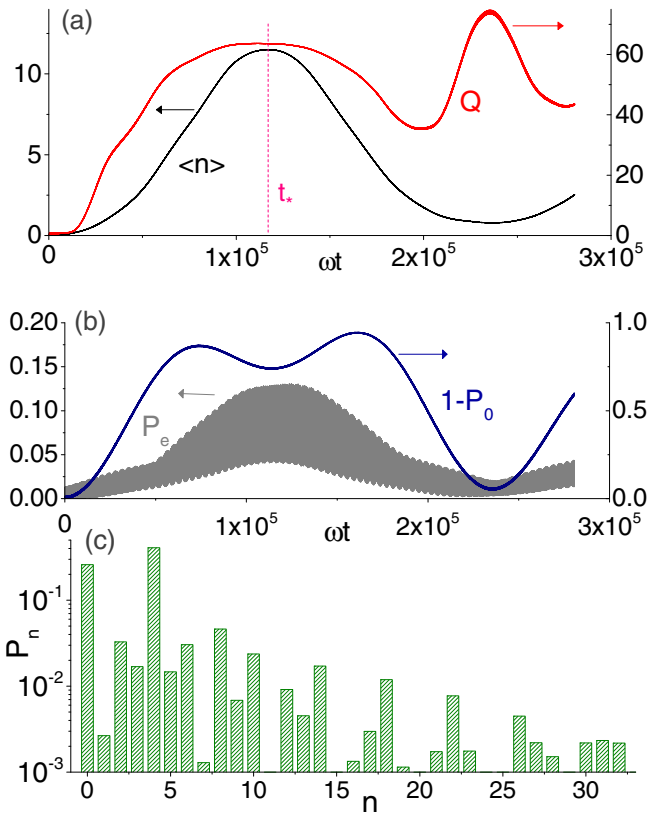

FIG. 2. (a) Average photon number $\langle n\rangle$ (scale on left axis) and the Mandel's Q factor (scale on right axis) as a function of time for the modulation of Kerr nonlinearity ($k = 2$). (b) Dynamics of the probabilities of atomic excitation P_e and nonvacuum photon states $1 - P_0$. (c) Photon number statistics at the time instant of maximum $\langle n\rangle$ [indicated by t_* in the panel (a)]. The values of all fixed parameters are given in the text.

the corresponding ratios for the standard DCE (i.e., for $k = 1$), for which $r_n = \sqrt{(n+1)(n+2)}/2$ does not depend on Ω. We see that the behavior of r_n is drastically different from that of the standard DCE, therefore, the dynamics will also be quite different. In Fig. 1(b) we plot the energy differences $\eta_n = \lambda_{n+2} - \lambda_n$ obtained by exact numeric diagonalization as a function of α/ω for $\Omega/\omega = 0.21$. For example, typical circuit QED experiments [42,58] employ cavity frequencies in the range of 5–15 GHz; the qubit frequencies lie in the range 1–10 GHz and can be tuned by as much as 1 GHz in 20 ns via external magnetic flux. We see that for $\alpha/\omega \approx 10^{-5}$ the spectrum becomes quasiharmonic, so it should be possible to generate several photons from vacuum for the modulation frequency $\eta \approx \eta_0$.

Figure 2 shows the dynamics obtained by solving numerically the Schrödinger equation with the original Hamiltonian (1) for the initial state $|\mathbf{0}, 0\rangle$ and parameters $k = 2$, $\Omega/\omega = 0.21$, $g/\omega = 0.07$, $\alpha/\omega = 10^{-5}$, $\varepsilon/\omega = 10^{-2}$, and $\eta/\omega = 2.0043$. Figure 2(a) shows the behavior of the average photon number $\langle n\rangle$ and the Mandel's factor $Q = [\langle(\Delta n)^2\rangle - \langle n\rangle^2]/\langle n\rangle$ (that quantifies the spread of the photon number distribution). Figure 2(b) shows the behavior of the atomic excitation probability P_e and the probability of occupation of

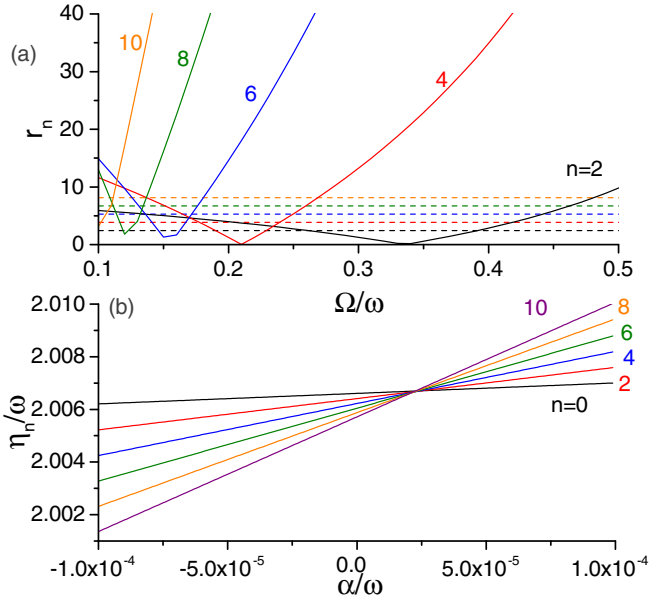

FIG. 3. Similar to Fig. 1 but for $k = 3$ (modulation of the third-order nonlinearity).

nonvacuum states of the field: $1 - P_0$, where $P_n = \mathrm{Tr}[|n\rangle\langle n|\hat{\rho}]$ is the n-photon probability and $\hat{\rho}$ is the total density operator. Figure 2(c) shows the photon statistics at the instant of maximum $\langle n\rangle$ (for the time $\omega t_* = 1.18\times10^5$). We see that several photons are generated, and the photon statistics is very different from the squeezed vacuum state that occurs for the standard cavity DCE. The qubit also becomes slightly excited during the photon generation process; this is easily explained by the fact that the modulation populates n-photon dressed states whose atomic weight is roughly $g^2 n/(\omega - \Omega)^2$ [see Eq. (10)].

Figure 3 is analogous to Fig. 1 but for $k = 3$ (all other parameters are the same). Once again we see that the behavior of r_n is quite different from the typical DCE scenario, and by properly adjusting the static Kerr nonlinearity α the spectrum can be made quasiharmonic [in Fig. 3(b) $\Omega/\omega = 0.31$]. The exact numeric dynamics is shown in Fig. 4 for parameters $k = 3$, $\Omega/\omega = 0.31$, $g/\omega = 0.07$, $\alpha/\omega = 2.5\times10^{-5}$, $\varepsilon/\omega = 10^{-2}$, and $\eta/\omega = 2.0067$. Figure 4(a) shows the behavior of $\langle n\rangle$ and Q, while Fig. 4(b) illustrates the dynamics of P_e, $1 - P_0$, and the largest probabilities of generation of n photons (other photon-number probabilities are significantly smaller). In this example, an even number of up to ten photons can be generated with significant probabilities.

Figures 2 and 4 demonstrate that in the presence of additional subsystems photons can be generated from vacuum due to the time modulation of cavity nonlinearities, but the dynamics is completely different from the standard cavity DCE.

III. EMPLOYING NONRESONANT CAVITY MODULATION

Now we consider a cavity whose frequency is modulated as $\omega(t) = \omega_0 + \varepsilon_\omega \sin\omega_1 t$, where $\omega_1 \neq 2\omega_0$, so that the resonant creation of quanta via DCE [2] does not take place. Adding the modulation of Kerr or higher nonlinearities, we have the

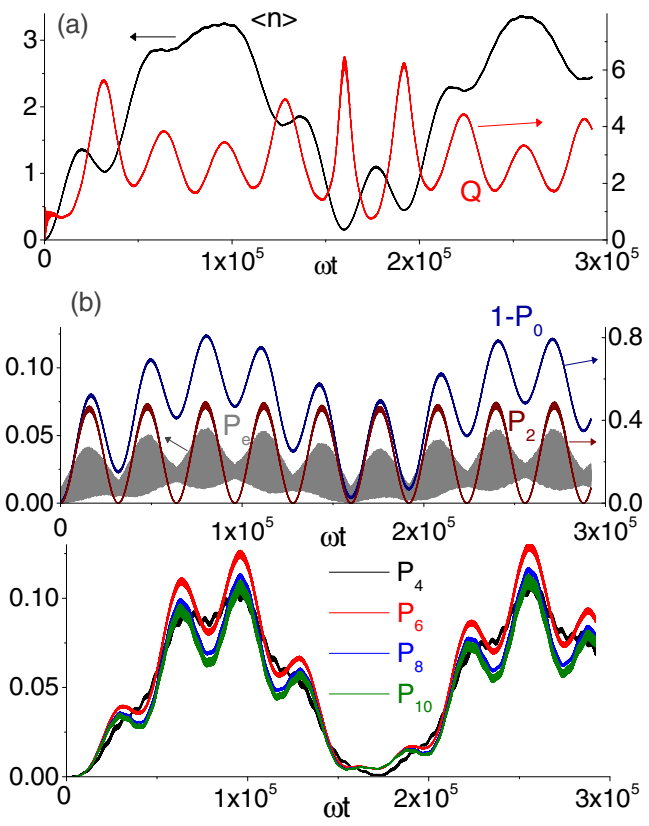

FIG. 4. Numeric dynamics for the modulation of the third-order nonlinearity ($k = 3$). (a) Average photon number and Mandel's factor. (b) Atomic excitation probability, nonvacuum excitation probability, and largest photon number probabilities as a function of time.

Hamiltonian (1) with the standard DCE contribution [55]

$$\hat{H}_0 = \omega(t)\hat{n} + i\frac{\dot{\omega}}{4\omega}(\hat{a}^{\dagger 2} - \hat{a}^2). \tag{14}$$

In the interaction picture defined by the unitary transformation

$$\hat{U} = e^{-iX(t)\hat{n}}, \quad X(t) = \frac{\varepsilon_\omega}{\omega_1}(1 - \cos\omega_1 t) + \frac{\omega_1 t}{2}$$

the Hamiltonian becomes

$$\hat{H}_0 = \zeta\hat{n} + \frac{2i\chi\cos\omega_1 t}{1 + (\varepsilon_\omega/\omega_0)\sin\omega_1 t}(\hat{a}^{\dagger 2}e^{2iX(t)} - \hat{a}^2 e^{-i2X(t)}),$$

where $\zeta = \omega_0 - \omega_1/2$ and $\chi = \varepsilon_\omega\omega_1/(8\omega_0)$. Using the Jacobi-Anger expansion, this Hamiltonian can be rewritten as a series of the Bessel functions with the argument $2\varepsilon_\omega/\omega_1$. However, under the realistic condition $\varepsilon_\omega \ll \omega_0, \omega_1$, we obtain to the first order in ε_ω

$$\hat{H}_0 \approx \zeta\hat{n} + 2i\chi\cos\omega_1 t(\hat{a}^{\dagger 2}e^{i\omega_1 t} - \hat{a}^2 e^{-i\omega_1 t}).$$

For low photon numbers n, given by the inequality $n\varepsilon_\omega \ll 10\omega_0$, one can neglect the rapidly oscillating terms $e^{\pm 2i\omega_1 t}$ to obtain

$$\hat{H}_0 \approx \zeta\hat{n} + i\chi(\hat{a}^{\dagger 2} - \hat{a}^2). \tag{15}$$

Expanding the wave function in terms of the eigenstates $|\varphi_n\rangle$ of Hamiltonian (15) as in Eq. (5), for $|R_{mn}| \ll \eta$ we obtain

$$\dot{c}_m \approx \sum_{n\neq m} e^{it\theta_{mn}(|\lambda_{nm}|-\eta)}\theta_{mn}R_{mn}c_n$$

with the transition rate R_{mn} given by Eq. (7).

For the realistic scenario $\chi n \ll |\zeta|$ for all relevant photon numbers n, the (non-normalized) eigenstates can be found from the nondegenerate perturbation theory as

$$|\varphi_n\rangle \approx |n\rangle - \frac{i\chi}{2\zeta}\left(\sqrt{\frac{(n+2)!}{n!}}|n+2\rangle + \sqrt{\frac{n!}{(n-2)!}}|n-2\rangle\right)$$
$$-\frac{\chi^2}{8\zeta^2}\left(\sqrt{\frac{(n+4)!}{n!}}|n+4\rangle + \sqrt{\frac{n!}{(n-4)!}}|n-4\rangle\right).$$

The transition rate becomes

$$R_{n,n+2} \approx i\varepsilon\frac{\chi}{4\zeta}\sqrt{(n+1)(n+2)}[(n+2)^k - n^k]$$
$$= i\varepsilon\frac{\chi}{\zeta}\sqrt{(n+1)(n+2)}M_k(n) \tag{16}$$

with $M_2(n) = n+1$ and $M_3(n) = 3n^2/2 + 3n + 2$. The eigenenergies read

$$\lambda_n \approx \zeta n - \frac{\chi^2}{\zeta}\left(1 + \frac{\chi^2}{\zeta^2}\right)(2n+1). \tag{17}$$

So for the modulation frequency

$$\eta = |\lambda_{n+2} - \lambda_n| \approx 2|\zeta|[1 - 2(\chi/\zeta)^2 - 2(\chi/\zeta)^4] \tag{18}$$

all the eigenstates become resonantly coupled (apart from the small shifts introduced by the neglect of rapidly oscillating terms [35]). In our case ζ can be both positive and negative, therefore DCE takes place whenever $\omega_1 \pm \eta \approx 2\omega_0$. We verified that for $\chi n \ll |\zeta|$ the approximate expressions (16) and (17) are in excellent agreement with the exact numeric diagonalization of the Hamiltonian (15).

We solved numerically the Schrödinger equation corresponding to the Hamiltonian (14). In Fig. 5(a) we illustrate the photon generation from the initial vacuum state $|0\rangle$ for the modulation of Kerr nonlinearity ($k = 2$) with parameters $\omega_1 = 5\omega_0$, $\varepsilon_\omega = 10^{-2}\omega_0$, $\varepsilon = 10^{-3}\omega_0$, and η given by Eq. (18). The panel on the top illustrates the behavior of $\langle n\rangle$ and Q, while the panel on the bottom illustrates the photon statistics at the time instant $\omega_0 t_* = 2.8\times10^5$. The long tail of the photon-number distribution explains the high value of the Q factor. In Fig. 5(b) we repeat the analysis for the modulation of the third-order nonlinearity with the modified parameters $\omega_1 = 0.7\omega_0$ and $\eta = 2|\zeta|[1 + 4(\chi/\zeta)^2]$. This figure attests that photons can be generated from vacuum via modulation of cavity nonlinearities even in the absence of additional subsystems, provided the cavity frequency is also modulated. In a sense, this is an interesting example of a positive "interference" between two different processes. Indeed, there is no photon generation in the standard DCE configuration with a high detuning of the wall vibration frequency in the absence of the Kerr medium; and no photon generation in the cavity at rest in the presence of a single Kerr nonlinearity. However, when two mechanisms are combined in a thoroughly thought

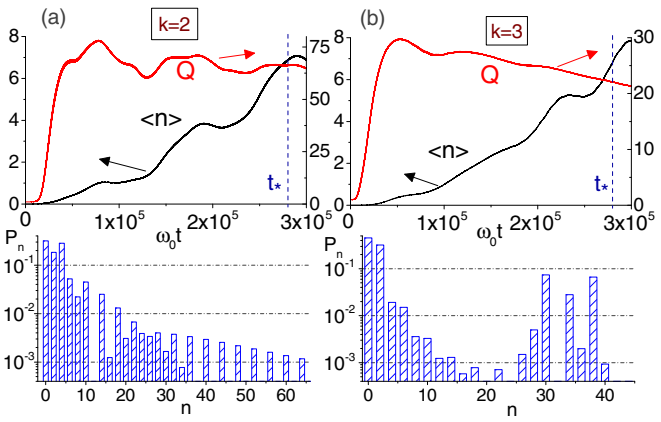

FIG. 5. (a) Simultaneous modulation of the Kerr nonlinearity and the cavity frequency for parameters $\omega_1 = 5\omega_0$ and $\eta \approx 2|\omega_0 - \omega_1/2|$. Top panel: $\langle n\rangle$ and Q as a function of time. Bottom panel: photon statistics at the time instant $t_* = 2.8\times 10^5\omega_0^{-1}$ (indicated by the vertical dashed line). (b) Similar analysis for the modulation of the third-order nonlinearity and $\omega_1 = 0.7\omega_0$.

out way, the generation becomes possible. Another example of such kind of "interference" connected with the Kerr medium was demonstrated in Ref. [60].

IV. DISCUSSION

Our results can be easily extended to other subsystems coupled to the cavity field and nonperiodic modulations, and they indicate that the photon generation from vacuum due to modulation of the nonlinear terms is possible. The peculiarity of this scheme is that the photon statistics is completely different from the squeezed vacuum state, since the transition rates grow much faster with n than for the parametric amplification process. The main disadvantages are the same as for other proposals of DCE, namely, the requirement of a large modulation amplitude and a finely tuned resonant modulation for a sufficiently long period of time. Since previous works predicted the photon generation from vacuum in cavity or circuit QED due to the modulation of cavity frequency, atomic frequency, or atom-field coupling strength, this work complements them by proving that under specific circumstances the modulation of cavity nonlinearities can also be employed to achieve generation of new states of light. The statistics of these states is *hyper-Poissonian* ($Q \gg 1$), similar to the states considered in Ref. [61]. Although the mean number of photons generated from vacuum in the schemes discussed above is not very big, probably, it could be increased after more thorough investigations of possible experimental realizations in the circuit QED arrangements. In any case, the discovery of a different kind of parametric DCE-like effects in nonlinear systems seems a significant achievement in the area of dynamical Casimir physics. Note that quite recently other mechanisms of nonlinear DCE were considered in Ref. [62].

ACKNOWLEDGMENT

Partial support from National Council for Scientific and Technological Development – CNPq (Brazil) is acknowledged.

[1] G. T. Moore, Quantum theory of the electromagnetic field in a variable-length one-dimensional cavity, J. Math. Phys. **11**, 2679 (1970).

[2] V. V. Dodonov, Nonstationary Casimir effect and analytical solutions for quantum fields in cavities with moving boundaries, in *Modern Nonlinear Optics*, Part 1, 2nd ed., edited by M. W. Evans, Advances in Chemical Physics Vol. 119 (Wiley, New York, 2001), p. 309.

[3] V. V. Dodonov, Current status of the dynamical Casimir effect, Phys. Scr. **82**, 038105 (2010).

[4] D. A. R. Dalvit, P. A. Maia Neto, and F. D. Mazzitelli, Fluctuations, dissipation and the dynamical Casimir effect, in *Casimir Physics*, edited by D. Dalvit, P. Milonni, D. Roberts, and F. da Rosa, Lecture Notes in Physics Vol. 834 (Springer, Berlin, 2011), p. 419.

[5] P. D. Nation, J. R. Johansson, M. P. Blencowe, and F. Nori, *Colloquium*: Stimulating uncertainty: Amplifying the quantum vacuum with superconducting circuits, Rev. Mod. Phys. **84**, 1 (2012).

[6] V. Dodonov, Fifty years of the dynamical Casimir effect, Physics **2**, 67 (2020).

[7] E. Yablonovitch, Accelerating Reference Frame for Electromagnetic Waves in a Rapidly Growing Plasma: Unruh-Davies-Fulling-Dewitt Radiation and the Nonadiabatic Casimir Effect, Phys. Rev. Lett. **62**, 1742 (1989).

[8] E. Yablonovitch, J. P. Heritage, D. E. Aspnes, and Y. Yafet, Virtual Photoconductivity, Phys. Rev. Lett. **63**, 976 (1989).

[9] V. I. Man'ko, The Casimir effect and quantum vacuum generator, J. Sov. Laser Res. **12**, 383 (1991).

[10] T. Okushima and A. Shimizu, Photon emission from a false vacuum of semiconductors, Jpn. J. Appl. Phys. **34**, 4508 (1995).

[11] Y. E. Lozovik, V. G. Tsvetus, and E. A. Vinogradov, Parametric excitation of vacuum by use of femtosecond laser pulses, Phys. Scr. **52**, 184 (1995).

[12] C. Braggio, G. Bressi, G. Carugno, A. Lombardi, A. Palmieri, G. Ruoso, and D. Zanello, Semiconductor microwave mirror for a measurement of the dynamical Casimir effect, Rev. Sci. Instrum. **75**, 4967 (2004).

[13] X.-D. Zhao, X. Zhao, H. Jing, L. Zhou, and W. Zhang, Squeezed magnons in an optical lattice: Application to simulation of the dynamical Casimir effect at finite temperature, Phys. Rev. A **87**, 053627 (2013).

[14] V. Hizhnyakov, A. Loot, and S. C. Azizabadi, Enhanced dynamical Casimir effect for surface and guided waves, Appl. Phys. A **122**, 333 (2016).

[15] E. Segev, B. Abdo, O. Shtempluck, E. Buks, and B. Yurke, Prospects of employing superconducting stripline resonators for studying the dynamical Casimir effect experimentally, Phys. Lett. A **370**, 202 (2007).

[16] T. Fujii, S. Matsuo, N. Hatakenaka, S. Kurihara, and A. Zeilinger, Quantum circuit analog of the dynamical Casimir effect, Phys. Rev. B **84**, 174521 (2011).
[17] G. R. Berdiyorov, M. V. Milošević, S. Savel'ev, F. Kusmartsev, and F. M. Peeters, Parametric amplification of vortex-antivortex pair generation in a Josephson junction, Phys. Rev. B **90**, 134505 (2014).
[18] A. V. Dodonov, Photon creation from vacuum and interactions engineering in nonstationary circuit QED, J. Phys.: Conf. Ser. **161**, 012029 (2009).
[19] J. R. Johansson, G. Johansson, C. M. Wilson, and F. Nori, Dynamical Casimir Effect in a Superconducting Coplanar Waveguide, Phys. Rev. Lett. **103**, 147003 (2009).
[20] J. R. Johansson, G. Johansson, C. M. Wilson, and F. Nori, Dynamical Casimir effect in superconducting microwave circuits, Phys. Rev. A **82**, 052509 (2010).
[21] C. M. Wilson, T. Duty, M. Sandberg, F. Persson, V. Shumeiko, and P. Delsing, Photon Generation in an Electromagnetic Cavity with a Time-Dependent Boundary, Phys. Rev. Lett. **105**, 233907 (2010).
[22] C. M. Wilson, G. Johansson, A. Pourkabirian, M. Simoen, J. R. Johansson, T. Duty, F. Nori, and P. Delsing, Observation of the dynamical Casimir effect in a superconducting circuit, Nature (London) **479**, 376 (2011).
[23] J. R. Johansson, G. Johansson, C. M. Wilson, P. Delsing, and F. Nori, Nonclassical microwave radiation from the dynamical Casimir effect, Phys. Rev. A **87**, 043804 (2013).
[24] P. Lähteenmäki, G. S. Paraoanu, J. Hassel, and P. J. Hakonen, Dynamical Casimir effect in a Josephson metamaterial, Proc. Natl. Acad. Sci. USA **110**, 4234 (2013).
[25] I.-M. Svensson, M. Pierre, M. Simoen, W. Wustmann, P. Krantz, A. Bengtsson, G. Johansson, J. Bylander, V. Shumeiko, and P. Delsing, Microwave photon generation in a doubly tunable superconducting resonator, J. Phys.: Conf. Ser. **969**, 012146 (2018).
[26] W. Wustmann and V. Shumeiko, Parametric resonance in tunable superconducting cavities, Phys. Rev. B **87**, 184501 (2013).
[27] A. L. C. Rego, H. O. Silva, D. T. Alves, and C. Farina, New signatures of the dynamical Casimir effect in a superconducting circuit, Phys. Rev. D **90**, 025003 (2014).
[28] J. Doukas and J. Louko, Superconducting circuit boundary conditions beyond the dynamical Casimir effect, Phys. Rev. D **91**, 044010 (2015).
[29] P. Corona-Ugalde, E. Martín-Martínez, C. M. Wilson, and R. B. Mann, Dynamical Casimir effect in circuit QED for nonuniform trajectories, Phys. Rev. A **93**, 012519 (2016).
[30] F. C. Lombardo, F. D. Mazzitelli, A. Soba, and P. I. Villar, Dynamical Casimir effect in superconducting circuits: A numerical approach, Phys. Rev. A **93**, 032501 (2016).
[31] C. Sabín, B. Peropadre, L. Lamata, and E. Solano, Simulating superluminal physics with superconducting circuit technology, Phys. Rev. A **96**, 032121 (2017).
[32] F. C. Lombardo, F. D. Mazzitelli, A. Soba, and P. I. Villar, Dynamical Casimir effect in a double tunable superconducting circuit, Phys. Rev. A **98**, 022512 (2018).
[33] S. Bosco, J. Lindkvist, and G. Johansson, Simulating moving cavities in superconducting circuits, Phys. Rev. A **100**, 023817 (2019).
[34] S. Ma, H. Miao, Y. Xiang, and S. Zhang, Enhanced dynamic Casimir effect in temporally and spatially modulated Josephson transmission line, Laser Photon. Rev. **13**, 1900164 (2019).
[35] A. V. Dodonov, Analytical description of nonstationary circuit QED in the dressed-states basis, J. Phys. A: Math. Theor. **47**, 285303 (2014).
[36] D. S. Veloso and A. V. Dodonov, Prospects for observing dynamical and anti-dynamical Casimir effects in circuit QED due to fast modulation of qubit parameters, J. Phys. B: At. Mol. Opt. Phys. **48**, 165503 (2015).
[37] S. Felicetti, C. Sabín, I. Fuentes, L. Lamata, G. Romero, and E. Solano, Relativistic motion with superconducting qubits, Phys. Rev. B **92**, 064501 (2015).
[38] I. M. de Sousa and A. V. Dodonov, Microscopic toy model for the cavity dynamical Casimir effect, J. Phys. A: Math. Theor. **48**, 245302 (2015).
[39] E. L. S. Silva and A. V. Dodonov, Analytical comparison of the first- and second-order resonances for implementation of the dynamical Casimir effect in nonstationary circuit QED, J. Phys. A: Math. Theor. **49**, 495304 (2016).
[40] D. Z. Rossatto, S. Felicetti, H. Eneriz, E. Rico, M. Sanz, and E. Solano, Entangling polaritons via dynamical Casimir effect in circuit quantum electrodynamics, Phys. Rev. B **93**, 094514 (2016).
[41] A. V. Dodonov, B. Militello, A. Napoli, and A. Messina, Effective Landau-Zener transitions in the circuit dynamical Casimir effect with time-varying modulation frequency, Phys. Rev. A **93**, 052505 (2016).
[42] X. Gu, A. F. Kockum, A. Miranowicz, Y.-X. Liu, and F. Nori, Microwave photonics with superconducting quantum circuits, Phys. Rep. **718-719**, 1 (2017).
[43] S. V. Remizov, A. A. Zhukov, D. S. Shapiro, W. V. Pogosov, and Yu. E. Lozovik, Parametrically driven hybrid qubit-photon systems: Dissipation-induced quantum entanglement and photon production from vacuum, Phys. Rev. A **96**, 043870 (2017).
[44] A. A. Zhukov, S. V. Remizov, W. V. Pogosov, D. S. Shapiro, and Yu. E. Lozovik, Superconducting qubit systems as a platform for studying effects of nonstationary electrodynamics in a cavity, JETP Lett. **108**, 63 (2018).
[45] H. Dessano and A. V. Dodonov, One- and three-photon dynamical Casimir effects using a nonstationary cyclic qutrit, Phys. Rev. A **98**, 022520 (2018).
[46] W. Wustmann and V. Shumeiko, Parametric effects in circuit quantum electrodynamics, Low Temp. Phys. **45**, 848 (2019).
[47] Y. N. Srivastava, A. Widom, S. Sivasubramanian, and M. P. Ganesh, Dynamical Casimir effect instabilities, Phys. Rev. A **74**, 032101 (2006).
[48] R. Román-Ancheyta, C. González-Gutiérrez, and J. Récamier, Influence of the Kerr nonlinearity in a single nonstationary cavity mode, J. Opt. Soc. Am. B **34**, 1170 (2017).
[49] A. Paredes and J. Récamier, Study of the combined effects of a Kerr nonlinearity and a two-level atom upon a single nonstationary cavity mode, J. Opt. Soc. Am. B **36**, 1538 (2019).
[50] L. A. Akopyan and D. A. Trunin, Dynamical Casimir effect in nonlinear vibrating cavities, Phys. Rev. D **103**, 065005 (2021).
[51] D. A. Trunin, Particle creation in nonstationary large N quantum mechanics, Phys. Rev. D **104**, 045001 (2021).
[52] R. H. Dicke, Coherence in spontaneous radiation processes, Phys. Rev. **93**, 99 (1954).
[53] B. M. Garraway, The Dicke model in quantum optics: Dicke model revisited, Philos. Trans. R. Soc. A **369**, 1137 (2011).

[54] A. V. Dodonov, Dynamical Casimir effect via four- and five-photon transitions using a strongly detuned atom, Phys. Rev. A **100**, 032510 (2019).

[55] C. K. Law, Effective Hamiltonian for the radiation in a cavity with a moving mirror and a time-varying dielectric medium, Phys. Rev. A **49**, 433 (1994).

[56] S. De Liberato, D. Gerace, I. Carusotto, and C. Ciuti, Extracavity quantum vacuum radiation from a single qubit, Phys. Rev. A **80**, 053810 (2009).

[57] A. F. Kockum, A. Miranowicz, S. De Liberato, S. Savasta, and F. Nori, Ultrastrong coupling between light and matter, Nat. Rev. Phys. **1**, 19 (2019).

[58] A. Blais, A. L. Grimsmo, S. M. Girvin, and A. Wallraff, Circuit quantum electrodynamics, Rev. Mod. Phys. **93**, 025005 (2021).

[59] B. L. Brock, J. Li, S. Kanhirathingal, B. Thyagarajan, W. F. Braasch, Jr., M. P. Blencowe, and A. J. Rimberg, Nonlinear Charge- and Flux-Tunable Cavity Derived from an Embedded Cooper-Pair Transistor, Phys. Rev. Appl. **15**, 044009 (2021).

[60] S. M. Chumakov, A. B. Klimov, and C. Saavedra, Competing interactions and quantum nonspreading wave packets, Phys. Rev. A **52**, 3153 (1995).

[61] A. V. Dodonov and V. V. Dodonov, Strong modifications of the field statistics in the cavity dynamical Casimir effect due to the interaction with two-level atoms and detectors, Phys. Lett. A **375**, 4261 (2011).

[62] D. A. Trunin, Nonlinear dynamical Casimir effect at weak nonstationarity, arXiv:2108.07747.